Conjunctival transcriptomics in ocular mucous membrane pemphigoid

Panthagani, Jesse; Suleiman, Kusy; Vincent, Rachel; Ong, Hon Shing; Wallace, Graham; Rauz, Saaeha

DOI:
10.1016/j.jtos.2023.09.005

Document Version
Publisher's PDF, also known as Version of record

Citation for published version (Harvard):
Panthagani, J, Suleiman, K, Vincent, R, Ong, HS, Wallace, G & Rauz, S 2023, 'Conjunctival transcriptomics in ocular mucous membrane pemphigoid', *The Ocular Surface*, vol. 30, pp. 142-149. https://doi.org/10.1016/j.jtos.2023.09.005

The Ocular Surface 30 (2023) 142–149

Contents lists available at ScienceDirect

The Ocular Surface

journal homepage: www.elsevier.com/locate/jtos

Conjunctival transcriptomics in ocular mucous membrane pemphigoid

Jesse Panthagani [a,b,1], Kusy Suleiman [a,b,1], Rachel C. Vincent [a], Hon Shing Ong [c,d,e], Graham R. Wallace [a,2], Saaeha Rauz [a,b,2,*]

[a] Academic Unit of Ophthalmology, Institute of Inflammation and Ageing, University of Birmingham, UK
[b] Birmingham and Midland Eye Centre, Sandwell and West Birmingham NHS Trust, Birmingham, UK
[c] Tissue Engineering and Cell Therapy Group, Singapore Eye Research Institute, Singapore
[d] Corneal and External Diseases Department, Singapore National Eye Centre, Singapore, Singapore
[e] Ophthalmology & Visual Sciences Academic Clinical Programme, Duke-NUS Medical School, Singapore

ARTICLE INFO

Keywords:
Inflammation
Fibrosis
Scarring
NanoString
ALDH1A3

ABSTRACT

Purpose: Ocular Mucous Membrane Pemphigoid (OcMMP) is an orphan disease characterized by chronic autoimmune-driven conjunctival inflammation leading to progressive scarring, debilitating symptoms, and blinding sequelae. This feasibility study aims to demonstrate conjunctival genetic transcriptomic analyses as a putative tool for interrogation of pathogenic signaling pathways in OcMMP.

Methods: Conjunctival RNA profiling using the NanoString nCounter Human Fibrosis panel was undertaken on RNA extracted from conjunctival swabs obtained from 6 MMP patients (8 eyes; 4 M/2F; median age 78 [range 64–84] years); and 8 age-matched control participants (15 eyes; 3 M/5F; median age 69.5 [range 69–88] years). Data from 770 genes were analyzed with ROSALIND HyperScale architecture and stratified according to the level of clinically visible bulbar conjunctival inflammation. Normalization, fold-changes ($\geq$+1.5-fold or $\leq$ −1.5-fold) and p-values adjustment (<0.05) using the Benjamini-Hochberg method were calculated.

Results: 93 differentially expressed genes (DEGs) were observed between OcMMP versus controls of which 48 were upregulated, and 45 downregulated. The top 4 upregulated DEGs represented fibrosis (COL3A1, COL1A1, FN1 and THBS1) while the key under-expressed genes (SCIN, HMGS2, XCL1/2) were indicative of ocular surface failure (goblet cell loss, keratinization, vulnerability to secondary infections). Forty-four pathways had a global significance score $\geq$2, the most significant being those related to extracellular matrix (ECM) remodeling, synthesis, and degradation. These pathways were accentuated in eyes with visible inflammation.

Conclusions: NanoString methodology acquired via a simple conjunctival swab identifies profibrotic genes in OcMMP group and differentiates inflamed eyes. Longitudinal sampling and following investigative intervention will further mechanistic insight and development of novel biomarkers to monitor disease progression.

1. Introduction

Mucous Membrane Pemphigoid is a group of hetereogenous autoimmune subepidermal blistering multisystem disorders that affects the skin and orificeal mucous membranes including the ocular (OcMMP), oral, aero-digestive tract, anogenital and genitourinary mucosae. OcMMP occurs in about 70% of cases and is typically characterized by a chronic relapsing conjunctival inflammation associated with a progressive scarring process that is bilaterally blinding in up to 20%, if left untreated [1,2]. While the prevalence of MMP is 1:40,000 [3], the incidence of ocular involvement ranges from 0.8 to 2.5 per million population [4,5]. The disease is more aggressive when it presents in younger populations [6]; early recognition and diagnosis is essential to reduce sight-threatening complications. Positive direct and/or indirect immunofluorescence studies detailing immunoprecipitation along the basement membrane zone (BMZ) are diagnostic of MMP with the exception of ocular monosite MMP, that can have negative immunofluorescence studies in 50% and more likely to have central corneal

* Corresponding author. Academic Unit of Ophthalmology, Birmingham and Midland Eye Centre, Institute of Inflammation and Ageing, College of Medical and Dental Sciences, University of Birmingham, Dudley Road, Birmingham, B18 7QU, United Kingdom.
E-mail address: s.rauz@bham.ac.uk (S. Rauz).
[1] Share the role of first author.
[2] Joint senior authors.

https://doi.org/10.1016/j.jtos.2023.09.005
Received 19 May 2023; Received in revised form 7 September 2023; Accepted 7 September 2023
Available online 9 September 2023

involvement and visual impairment [7–9].

The ocular features are characterized by chronic autoimmune-driven conjunctival inflammation leading to progressive scarring, debilitating symptoms and blinding sequelae. Systemic immunotherapy is the mainstay and modifies inflammation but does not limit progression of fibrosis either in inflamed eyes, or in 50% of clinically quiescent eyes. Progression of fibrosis results in trichiasis, lid malposition, severe dry eye, keratinization, ocular surface failure and recurrent infections leading to irreversible blindness. Understanding the pathogenic mechanism underpinning progressive conjunctival fibrosis is essential to facilitate development of novel anti-scarring therapies for which there is a clear unmet clinical need. The pathogenesis includes loss of tolerance to conjunctival mucosal epithelial BMZ proteins resulting in the development of pathogenic autoreactive T cells that trigger antibody (IgG, IgA) production from plasma cells to the BMZ. Antibody-BMZ interaction activates the complement cascade, acute inflammation, accumulation of inflammatory effector cells (neutrophils, dendritic cells, mast cells, eosinophils, macrophages) and associated cytokines/growth factors (IL2, IL5, IL13, IFNγ,TNFα) resulting in expansion of both Th1 and Th2 cells in the chronic inflammatory-fibrotic phase of OcMMP. Autoreactive T cells may mediate an antibody-independent pathway with similar effects [10,11].

Macrophages, T cells, mast cells and eosinophils release profibrotic mediators (PDGF, IL-13, TGFβ and HSP47). In addition, dendritic cell aldehyde dehydrogenase (ALDH1A3) catalyzes retinaldehyde to retinoic acid which in turn activates conjunctival fibroblasts leading to extracellular matrix deposition (e.g. Type 1 and 3 collagen, fibronectin, thrombospondin). Fibroblasts release proinflammatory and profibrotic factors (IL-1, IL-6, VEGF) perpetuating the chronic inflammatory response [12–14]. Furthermore, pemphigoid fibroblasts remain profibrotic after clinical inflammation resolves, through an autocrine ALDH-mediated retinoic acid effect driving conjunctival fibrosis [11,15]. i.e. during both active inflammation and after resolution, the activated OcMMP fibroblasts continue to scar. The induction of the TGFβ1 gene, and/or activation of latent TGFβ1 seem to play an important role [10]. TGFβ driven critical changes in fibroblast metabolism in addition with pro-inflammatory cytokines and growth factors lead to an activation to a myofibroblast phenotype, and extracellular matrix production (ECM) formation and remodeling in fibrosis and NGF/$p75^{NTR}$ may have a role to play in early fibrosis [16,17]. Ultimately, total ocular surface failure results from extreme dry eye, often complicated by recurrent infection, and leading to surface keratinization.

More objective biomarkers are required to identify fibrosis signaling pathway and associated inflammatory cascade activity. As longitudinal conjunctival tissue biopsy is not feasible and not considered acceptable to patients, the main objective for this pilot study was to optimize a and test the feasibility of a relatively non-invasive conjunctival swab sampling technique used in combination with the NanoString platform to phenotype the global conjunctival transcriptome comprising several hundred genes in healthy subjects and OcMMP patients. Interrogation of the differential gene expression of the conjunctival transcriptome may provide insight into new targets for anti-fibrotic therapy, and guide clinical decision-making for initiation, maintenance, and withdrawal of immunosuppressive, and when available, anti-scarring therapies.

2. Methods

2.1. Ethics statement

Clinical data collection and patient sampling were undertaken after informed written consent from each study participant following the tenets of the Declaration of Helsinki and approval by the Health Research Authority Ethics Committee (Inflammation in Ocular Surface Disease (IOSD); Reference: 08/H1206/165 UKCRN 7448).

2.2. Study subjects and clinical data

Fourteen participants were recruited from the ocular surface disease and cataract clinics presenting to the Birmingham & Midland Eye Centre, Birmingham, UK. Diagnosis of OcMMP was based on clinical findings characteristic for the disease: progressive conjunctival cicatrization in the absence of other causes of conjunctival scarring (n = 6 [8 eyes]; 4 M/2F; median age 78 [range 64–84; mean 76.4] years); with five patients' direct immunofluorescence positive of whom three were also indirect immunofluorescence positive). Tissue biopsy immunofluorescence status was defined as positive by the presence of a linear deposition of IgG, IgA, or complement (C3) along the BMZ, and negative if typical clinical characteristics were evident with a negative a immunofluorescence status (because of the recognition of a subgroup of ocular mono-site patients who have ocular features consistent with OcMMP but have a negative biopsy) [8,9]. Indirect immunofluorescence positive was defined as the presence of patient serum IgA or IgG binding to salt split skin or monkey oesophagus substrates. Cross-sectional comparisons were made with a group of healthy, age-matched control subjects (n = 8 [15 eyes]; 3 M/5F; median age 69.5 [range 69–88; mean 73.1] years) defined as subjects with no history or clinical evidence of ocular, systemic inflammatory, or autoimmune disease (including dry eye), contact lens wear, previous ocular surgery, cataract surgery within three months, or use of topical ophthalmic medication. These patients were identified from new patients presenting to the nurse-led cataract clinics (hypertensive, 3; osteoporosis, 1; and no ocular or systemic comorbidities, 4).

All OcMMP patients underwent a detailed examination including the Ocular Surface Disease Index (OSDI®; Allergan-Abbvie) self-administered symptom questionnaire, the Cicatrising Conjunctivitis Assessment Tool (CCAT®) a validated tool for measuring progressive conjunctival fibrosis comprising three domains: inflammation (an indicator of disease activity), scarring and morbidity (both indicators of disease damage) [18] and the SICCA Ocular Staining Score (OSS) [19]. Healthy controls were recruited from patients referred from community optometrists for consideration of cataract surgery.

2.3. Sample collection and RNA extraction

Conjunctival swabs were obtained from the lower conjunctival fornix from 6 patients (8 eyes) with a diagnosis of OcMMP and from 8 healthy age-matched patients (15 eyes) with cataract. The swab procedure involved anesthesia using proxymetacaine 0.5% eye drops instilled in both eyes. After 30 s, a Puritan™ sterile standard foam tipped applicator was used to sweep the inferior fornix six times and placed directly into a 1.5 ml microcentrifuge tube containing 1 ml TriReagent, a component from the RiboPure™ RNA purification kit (Thermo Scientific, Waltham MA, USA). The redundant swab stick was cut with sterile scissors, the microfuge tube closed and vortexed at maximum speed for 1 min. After a 5-min incubation at room temperature, the homogenized sample was transferred to a −80 °C freezer until further analysis. Total RNA was isolated following the RiboPure™ RNA purification and elution manufacturer's protocol (Thermo Scientific, Waltham MA, USA) giving a total volume of 30 μL. RNA concentration, integrity and purity were quantified with spectrophotometery (NanoDrop 2000™), Qubit™ 2.0. Fluorometer (Thermo Scientific, Waltham MA, USA) and the Agilent Bioanalyzer (Agilent, Santa Clara CA, USA).

2.4. NanoString and data analysis

The NanoString nCounter® multiplexed target platform using the Human Fibrosis panel (https://nanostring.com/) quantified 770 genes. nCounts of mRNA transcripts were normalized using the geometric means of 10 housekeeping genes (ACAD9, ARMH3, CNOT10, GUSB, MTMR14, NOL7, NUBP1, PGK1, PPIA and RPLP0). Data were analyzed using ROSALIND (https://rosalind.bio/), with a HyperScale architecture developed by ROSALIND, Inc. (San Diego, CA). Read Distribution percentages, violin plots, identity heatmaps, and sample MDS plots were generated as part of the quality control step. Normalization, fold changes and p-values were calculated using criteria provided by NanoString. ROSALIND follows the nCounter Advanced Analysis protocol of dividing counts within a lane by the geometric mean of the normalizer probes from the same lane. Housekeeping probes to be used for normalization are selected based on the geNorm algorithm as implemented in the NormqPCR R library[200]. The abundance of various cell populations was calculated on ROSALIND using the NanoString Cell Type Profiling Module. ROSALIND performs a filtering of Cell Type Profiling to include results that have scores with a p-value $\geq$0.05. Fold changes and p-values were calculated using the fast method as described in the nCounter Advanced Analysis 2.0 User Manual. The Gene Set Analysis (GSA) module from NanoString is incorporated into ROSALIND to summarize the global significance score and the directed global significance score. GSA summarizes the change in regulation within each defined gene set relative to the baseline, as described in the manufacturer's manual. The values calculated are the global significance score which measure the overall differential expression of the selected gene set relative to selected patient populations, ignoring whether each gene is up- or down-regulated.

P-value adjustment is performed using the Benjamini-Hochberg method of estimating false discovery rates (FDR). Clustering of genes for the final heatmap of differentially expressed genes was performed using the PAM (Partitioning Around Medoids) method using the fpc R library [211] that takes into consideration the direction and type of all signals on a pathway, the position, role and type of every gene. Hypergeometric distribution was used to analyze the enrichment of pathways, gene ontology, domain structure, and other ontologies. The topGO R library was used to determine local similarities and dependencies between GO terms in order to perform Elim pruning correction. Several database sources were referenced for enrichment analysis, including Interpro [20], NCBI [21], MSigDB [22,23], REACTOME [24], WikiPathways [25]. Enrichment was calculated relative to a set of background genes relevant for the experiment. Data and graphs analyzed in ROSALIND were downloaded including Volcano plots of differential expression data (plotted using the −log10 (p-value) and log2 fold change and heat maps.

Comparisons of OcMMP patients with OSDI®, CCAT© and OSS scores were performed using the Spearman rank test using GraphPad Prism version 9.0 (San Diego, CA, USA).

3. Results

3.1. Patient characteristics

OcMMP patient characteristics are summarized in Table 1. Three eyes (3 patients) showed minimal inflammation defined as a score of 0–1 (Max) 20 using the inflammation domain of the cicatrising conjunctivitis assessment tool (CCAT©), and inflamed eyes with a score of 4–20 (max 20).

3.2. Differentially expressed genes in OcMMP patients versus controls

Out of the 760 genes (excluding housekeeping genes) included in the NanoString Fibrosis Panel, there were a total of 93 differentially expressed genes (DEGs) with 48 upregulated genes and 45 downregulated genes. These are displayed in the volcano plot shown in Fig. 1A with a fold change of 1.5 used to compare the different subject groups [26] with a -log10 adjusted p-value of 0.05 with specific upregulated and downregulated DEGs displayed in Supplementary Tables S1 and S2, respectively (Quantity and quality of RNA is detailed in Supplementary Table S4 and The Full 770 gene codeset with up and down regulated genes can be found **Supplementary S5.**).

3.3. Differentially expressed pathways

The DEGs identified were used to assess 51 specific pathways that may be involved using the NanoString and ROSALIND software. Differential expression analysis is calculated using a t-statistic for each gene against each covariate in the model. The top 20 pathways are highlighted in Fig. 1B. For each pathway, the number of unaffected and modulated are highlighted. The top twelve genes (COL3A1 and COL1A1, FN1, THBS1, TPSAB1/B2, SERPINE1, SPP1, COL5A1, OASL, IL1B, ANGPTL4, LAMA3) represented upregulation of extracellular matrix remodeling and synthesis, (4.807), collagen biosynthesis and modification (4.343) and extracellular matrix degradation (3.768). The main under-expressed genes that have relevance to mucosal health secondary to fibrosis including SCIN (fundamental goblet cell mucin secretion), HMGS2 (mitochondrial metabolic enzyme), and XCL1/2 (antimicrobial actions). Heat maps showing DEGs within these and other pathways are shown in Fig. 2. Importantly, OcMMP inflamed eyes (n = 5) showed a greater expression of not only COL1A1, COL3A1, but also other genes including FN1, SPP1, COL5A1, LAMA3, LAMC1 and NID1 when compared to OcMMP eyes with minimal or no inflammation. In addition, neural cell adhesion molecule (NCAM1, CD56) integrin subunit alpha 1 (ITGA1, CD49d) and KLKB1 (prekallikrein) were all downregulated in patients with OcMMP (Fig. 2A) regardless of the inflammation status of individual eyes. This would suggest a decrease in neural trafficking within ocular tissue in these eyes. In the cytokine panel (Fig. 2B), genes encoding proteins associated with the IL-1 pathway, IL-1β, IL-18, IL-33 and IL1RAP, a ligand for IL-33, were upregulated in OcMMP eyes associated with inflammation. By comparison, genes associated with the adaptive immune response CXCR3, CXCR6, LTA, LTB and IL12RB were all upregulated in healthy eyes (i.e., downregulated in OcMMP eyes). Type 1 interferon panel showed a strong increase in genes associated with interferon and anti-viral function such as 2,5 oligodenylate synthase (OASL, OAS1), and interferon inducible proteins (IFI6, IFI27) in OcMMP non-inflamed eyes, whereas inflamed eyes had reduced expression compared to healthy eyes.

In the PDGF signaling panel (Fig. 2C), genes encoding proteins relating to cell proliferation and increased extracellular matrix deposition (COL3A1, COL5A1 and THBS1) were upregulated in OcMMP eyes associated with inflammation. Interestingly, CTSW (Fig. 2C – Platelet degranulation panel), a gene that has specific function in regulating cytotoxic activity of both cytotoxic T-cells and NK cells, was found to be downregulated in OcMMP eyes (and upregulated in healthy controls).

The cholesterol panel showed an overall upregulation of genes associated with lipid metabolism in OcMMP. Of note, angiopoietin like 4 (ANGPTL4), a gene known to also encode for an apoptosis survival factor, is also upregulated in OcMMP.

Fig. 2D highlights other upregulated genetic pathways, namely:

Table 1
OcMMP patient characteristics.

		Eyes with Active Inflammation					Eyes with Inactive Inflammation		
Patient Demographics	Patient Number	1		2		3	4	5	6
	Age (Years)	78		81		64	78	84	74
	Gender (M/F)	M		F		M	M	F	M
	Eye Laterality (R/L)	R	L	R	L	R	L	L	L
Visual Acuity	LogMAR	0.8	0.3	0.5	0.2	0.1	0.2	0.4	0.2
Biopsy	DIF	Positive	Positive	Positive	Positive	Positive	Positive	Positive	Negative
	IIF	Negative		Positive		Negative	Positive	Positive	Negative
	Overall biopsy status	Positive		Positive		Positive	Positive	Positive	Negative
OSDI	**Total Score (0–100)**	**75**		**50**		**0**	**15.9**	**0**	**6.25**
SICCA OSS	**Total Score (0–12)**	**5**	**9**	**1**	**1**	**2**	**1**	**2**	**6**
Conjunctival Inflammation	Bulbar Conjunctival Hyperaemia (0–16)	4	4	8	6	5	0	0	1
	Limbitis Score (0–4)	0	1	4	4	0	0	0	0
	Total Inflammation Score (0–20)	**4**	**5**	**12**	**10**	**5**	**0**	**0**	**1**
Conjunctival Scarring	Subconjunctival Fibrosis	Yes	Yes	Yes	Yes	Yes	Yes	Yes	Yes
	Lower Fornix Symblepharon (Score)	<50%	<50%	≥50%	≥50%	<50%	<50%	<50%	≥50%
	Upper Fornix Symblepharon (Score)	Absent	Absent	<50%	<50%	<50%	Absent	Absent	≥50%
	Total Fornix Symblepharon Score (0–4)	**1**	**1**	**3**	**3**	**2**	**1**	**1**	**4**
Morbidity	Distichiasis Presence	No	No	Yes	Yes	Yes	No	No	No
	Keratinization	No	No	Yes	Yes	No	No	No	Yes
	Corneal Vascularization Score (0–5)	0	1	2	0	0	0	0	0
	Corneal Scarring Score (0–9)	5	1	0	0	0	0	0	0
	Total Morbidity Score (0–14)	**5**	**2**	**2**	**0**	**0**	**0**	**0**	**0**

Table 1: **Summary of clinical data of OcMMP patients**. Conjunctival inflammation, conjunctival scarring and morbidity form 3 domains from the cicatrising conjunctivitis assessment tool (CCAT© (i) inflammation = bulbar hyperaemia each quadrant graded on a 5-point (0–4) scale and limbitis, number of involved quadrants (0–4); (ii) Scarring = subconjunctival fibrosis, yes/no; symblepharon, absent (0), <50% (1), >50% (2); central upper and lower forniceal depth if performed with a fornix depth measurer; (iii) Morbidity = Distichiasis, yes/no; Keratinization, yes/no; corneal vascularization and opacity, each peripheral corneal quadrant involved (scored 1), central cornea vessels (1), total vessels score = 5, central corneal opacity (5), total opacity score = (9) for involvement by vessels or opacity separately). (**Abbreviations:** M, male; F, female; R, right; L, left; OSDI, ocular surface disease index score; SICCA OSS, SICCA ocular staining score).

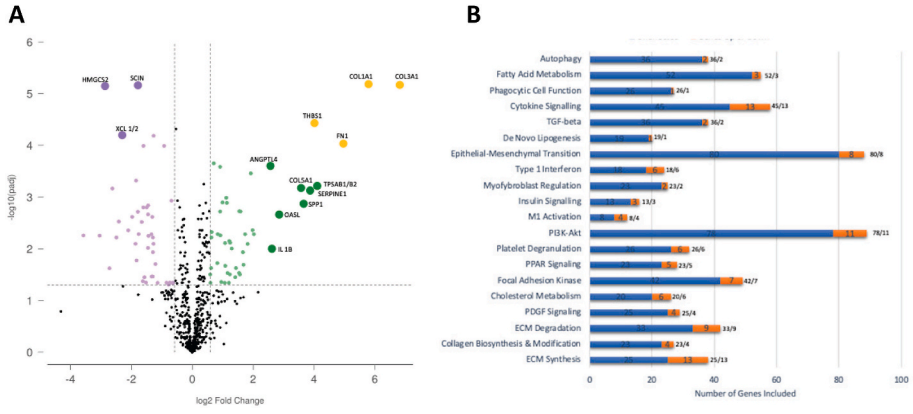

Fig. 1. (Panel A) Differential expression of genes in the conjunctiva of OcMMP eyes. A volcano plot shows -log10(p-value) and log 2-fold change in gene expression in OcMMP compared to matched control eyes (fold increase >1.5 or fold decrease <1.5 and p adjusted value of 0.05). P-value thresholds were adjusted using the Benjamini-Hochberg method of estimating false discovery rates. The horizontal line indicates p = 0.05, and the two vertical lines indicate greater or lower than 1.5-fold. Genes highlighted in orange are representative of profibrotic pathways (note top two genes are Collagen Types I and 3) and under-expressed genes (in purple) are representative of ocular mucosal failure. (**Panel B**) Gene set analysis pathway descriptors. Orange bars indicate modulated genes (up or down), and blue bars show unaffected genes. Numbers adjacent to the bars indicate the number of unaffected genes (left) followed by the affected genes (right).

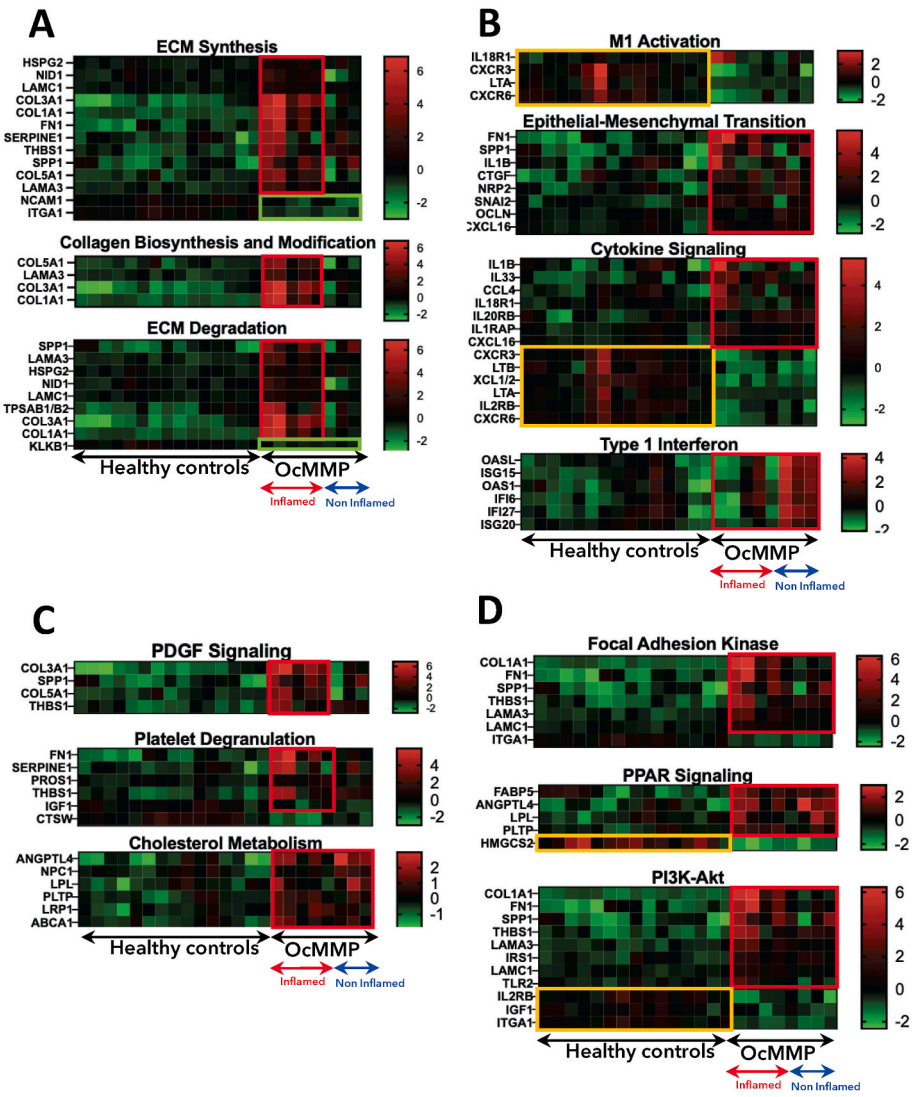

Fig. 2. Heatmaps of the fibrosis pathway expression with global significance scores in pemphigoid versus control eyes. (**Panel A**) The key upregulated genes in OcMMP eyes that have clinically graded active inflammation are related to extracellular matrix (ECM) synthesis, collagen biosynthesis and modification, and ECM degradation. While **Panel B** shows upregulation of select inflammatory cytokine and epithelial-mesenchymal transition profile in OcMMP eyes independent of clinical grading of inflammation. M1 activation and adaptive immune response cytokines and chemokines were upregulated in control eyes representative of an 'active' protection role; whereas innate response cytokines were associated with diseased eyes. Differentiation between OcMMP versus control eyes were also seen in other pathways including PDGF signalling, platelet degranulation, cholesterol metabolism, focal adhesion kinase, PPAR signalling and PI3K-Akt signalling pathways (**Panels C and D**). (**Key**: red box, OcMMP upregulated genes; green box, OcMMP downregulated genes; orange box, control upregulated genes).

Focal adhesion kinase, PPAR signaling and PI3K-Akt pathways. Interestingly, Toll like receptor 2 (TLR2), strongly involved in activation of the innate immune system in response to pathogen recognition, was upregulated in inflamed OcMMP eyes. Such upregulation in TLR activity has previously been implicated in the pathogenesis of several autoimmune diseases. By contrast, Insulin-like growth factor (IGF-1) expression involved in epithelial cell migration and healing, was strongly upregulated in healthy eyes versus all OcMMP eyes.

3.4. *Correlation of DEGs with clinical scoring systems*

Correlation analysis between the normalized counts versus the OSDI© symptom and the CCAT® conjunctival inflammation score was performed to investigate whether DEGs were associated with clinical outcome measures. Out of the 93 DEGs, 16 DEGs correlated with either the OSDI® or CCAT© scores. No DEGs correlated with both scoring systems.

The OSDI® symptom score positively correlated with upregulation of COL1A1 and LAMC1 representative of increasing symptomatology with increasing fibrosis and extracellular matrix deposition (Table 2) [27,28]. Conversely, the presence of symptoms and a higher OSDI score was negatively correlated with KLRB1, SH2D1A, KLRK1, CXCR6, CD3D and PRKACB gene expression. These genes represent stimulation, activation, signal transduction, development and regulation of T-cell populations, indicative of attenuation of the adaptive immune response in patients with a higher level of reported symptoms (Table 2) [29–34].

On analyzing DEG against the CCAT© inflammation domain score, upregulation of PSMC3, PANX1, NPC1 and OCLN together with the downregulation of KIR2DL3, all negatively correlated with inflammation. Collectively the genes maintain an intact conjunctival mucosal epithelial barrier, or normalization of anatomy after an inflammatory response (Table 3) [35–39]. By contrast, increasing conjunctival inflammation was positively correlated with downregulation of RNF152, EEF2K, and TCF7L1: genes involved in the inflammation-fibrosis signaling axis (Table 3) [40–42]. There was no statistical significance in the gene readouts and ocular staining sicca (OSS) scores (data not shown).

Table 2
Correlation of DEGs with OSDI® patient-reported score.

Expression Change	Gene	Gene Name	Gene Role	OSDI Correlation
Upregulated Genes	COL1A1	Collagen Type I Alpha 1 Chain	Encodes the pro-alpha1 chains of type I collagen, which is found in most connective tissues and is abundant in bone, cornea, dermis and tendon [27].	0.7638*
	LAMC1	Laminin Subunit Gamma 1	Encodes a subunit protein for an extracellular matrix glycoprotein. It is implicated in an array of biological processes including cell adhesion [28].	0.7638*
Downregulated Genes	KLRB1	Killer Cell Lectin Like Receptor B1	Encodes for a type II membrane protein involved in regulation of NK cell function [29].	−0.9092**
	SH2D1A	SH2 Domain Containing 1A	Encodes a protein that plays a major role in the bidirectional stimulation of T and B cells [30].	−0.8486*
	KLRK1	Killer Cell Lectin Like Receptor K1	Encodes for a transmembrane receptor protein (type II membrane orientation - It binds to a diverse family of ligands that include MHC class I chain-related A and B proteins and UL-16 binding proteins, which may lead to activation of NK and T cells [31].	−0.8244*
	CXCR6	C-X-C Motif Chemokine Receptor 6	Encodes a G protein-coupled chemokine receptor expressed in several T lymphocyte subsets and bone marrow stromal cells. Binds chemokine ligand 16 (CCL16), regulates T lymphocyte migration to peripheral tissues [32].	−0.9456*
	CD3D	CD3 Delta Dubunit Of T-cell Receptor Complex	Encodes a membrane protein which is part of the T-cell receptor/CD3 complex (TCR/CD3 complex) and is involved in T-cell development and signal transduction [33].	−0.8244*
	PRKACB	Protein Kinase cAMP-Activated Catalytic Subunit Beta	Encodes a member of the serine/threonine protein kinase family. The encoded protein is a catalytic subunit of cAMP (cyclic AMP)-dependent protein kinase, which mediates signalling though cAMP [34].	−0.7395*

Table 2: DEGs significantly correlated with patient symptomatology scores (measured by the OSDI® symptom score; Spearman rank coefficient of correlation. *P < 0.05, **P < 0.01).

Table 3
Correlation of DEGs with the CCAT© inflammation domain.

Expression Change	Gene	Gene Name	Gene Role	CCAT Correlation
Upregulated Genes	PSMC3	Proteasome 26S Subunit, ATPase 3	Encodes proteosome sub-units and degrades ubiquitin modified proteins. Encodes proteosome sub-units and degrades ubiquitin modified proteins [35].	−0.9157**
	PANX1	Pannexin 1	Innexin family gap junction gene, protein of which abundantly expressed in central nerve system (CNS). Potential biomarker for immune infiltration (in pancreatic cancer [36].	−0.9157**
	NPC1	NPC Intracellular Cholesterol Transporter 1	Encodes large protein in limiting membrane of endosomes and lysosomes. Mediates intracellular cholesterol trafficking - transports low-density lipoproteins to late endosomal/lysosomal compartments where they are hydrolysed and released as free cholesterol [37].	−0.7952*
	OCLN	Occludin	Encodes an integral membrane protein necessary for cytokine-induced regulation of the tight junction paracellular permeability barrier [38].	−0.8675**
Downregulated Genes	KIR2DL3	Killer Cell Immunoglobulin Like Receptor, Two Ig Domains and Long Cytoplasmic Tail 3	Encodes transmembrane glycoproteins expressed by NK cells and a subset of T-cells. Involved in transducing inhibitory signals upon ligand binding [39].	−0.8193*
	RNF152	Ring Finger Protein 152	Located in lysosomal membrane, the coded protein enables small GTPase binding and ubiquitin protein ligase activity [40].	0.7711*
	EEF2K	Eukaryotic Elongation Factor 2 Kinase	Encodes highly conserved protein kinase in the calmodulin-mediated signalling pathway [41].	0.8434*
	TCF7L1	Transcription Factor 7 Like 1	Encodes a member of the T cell factor/lymphoid enhancer factor family of transcription factors. activated by beta-catenin, mediate Wnt signalling, and antagonized by TGF-B signalling pathways [42].	0.8555*

Table 3: DEGs significantly correlated with conjunctival inflammation scores (CCAT® inflammation domain; Spearman rank coefficient of correlation. *P < 0.05, **P < 0.01).

4. Discussion

Using a simple conjunctival swabbing sampling technique from the inferior fornix without the need of expensive consumables or incisional tissue biopsy, we have been able to use the NanoString platform and the fibrosis panel to identify 93 differentially expressed genes (DEGs) when comparing OcMMP and healthy participant eyes. Of these, 48 DEGs were upregulated, and 45 were downregulated. The top four upregulated DEGs represented genes known to be involved in the OcMMP conjunctival fibrosis pathway (COL3A1, COL1A1, FN1 and THBS1), whereas the key under expressed genes (SCIN, HMGS2, XCL1/2) were indicative of ocular surface failure (goblet cell loss, keratinization, vulnerability to secondary infections). Moreover, changes in expression of cytokine genes associated with innate or adaptive immunity correlated with clinical activity (patient symptomatology and clinically graded inflammation) in OcMMP eyes.

Murine studies of dry eye disease have utilized NanoString technology mouse immunology panel identifying specific RNA transcripts in mice treated with tyrosine kinase agonist in a desiccating stress model [43]. In a similar model, NanoString immune arrays were performed on sorted $MHCII^{+}$ and $MHCII^{-}$ monocyte/macrophage cell populations. The results showed an increase in transferred myeloid cells and decrease in resident myeloid cells. Genes associated with antigen presentation, cytokine/chemokine, M1 macrophage and NLRP3 inflammasome pathways were increased supporting an increase in innate immunity which may be involved in lacrimal gland dysfunction [44]. A study to investigate specific signaling pathways in two experimental mouse dry eye (EDE) models, kept animals in a controlled desiccative environment.

Two groups, one treated with scopolamine and second subjected to extra orbital lacrimal gland excision bilaterally identified in different altered gene transcripts although functional annotation analysis revealed that the same inflammatory pathways were involved in both models [45]. These murine studies supported an inflammatory response in dry eye disease.

In human studies using the nCounter® Human inflammation v2 codeset that enables multiplexing for over 200 inflammation genes, bulbar conjunctival superficial cells collected by impression cytology using a 13 mm Supor200® PES Membrane Disc Filters (0.2 μM) from patients with primary Sjögren's syndrome (n = 30 eyes, control eyes = 15) supported the earlier mouse findings with 27 genes increased and 13 decreased expression in Sjögren's eyes compared with controls. Several altered genes (n = 14) correlated with OSDI® patient symptom score and the corneal function score. IL1RN was the only gene that positively correlated with a reduction in Schirmer test [46]. In a second study, EyePrim™ impression cytology samples from the temporal conjunctiva from Sjögren's eyes (n = 7; versus 19 control eyes) were analyzed using the Human Immunology V2 panel examining 594 genes showed 53 DEGs (49 increased and 4 decreased). Several DEGs showed a correlation with clinical parameters such as the tear film break up time [26]. These human studies further support an inflammatory phenotype gene expression in the conjunctiva in complex dry eye pathogenesis, that can be detected by performing impression cytology (avoiding surgical incisional biopsy).

In our study, using the NanoString Fibrosis Panel that profiles 770 genes across 51 annotated pathways, we have phenotyped autoimmune-driven progressive conjunctival scarring in OcMMP patients (8 eyes) versus aged-matched control eyes (n = 15) using a simple inferior conjunctival fornix swab technique. We demonstrated the most important pathways were related to ECM synthesis and degradation together with collagen biosynthesis and modification. While we did not perform qPCR, protein ELISA or tissue biopsy immunohistochemistry to validate the NanoString readouts, our data confirmed overexpression of COL1A1 and COL3A1 genes. This was in keeping with previous published studies that used immunohistochemical analyses of conjunctival mucosal tissue and primary fibroblast culture derived from conjunctival biopsies [16,47,48]. The overproduction of ECM by myofibroblasts results in an unorganized deposition of type I and III collagen protein leading to fibrosis and, eventually, scar formation.

Profibrotic mediators such as PDGF [49], IL-13,[14] TGFβ [50], and HSP47 [48] (heat shock protein) released by macrophages, T cells, mast cells and eosinophils also have direct effects on fibroblasts. Further, SPP1, a gene associated with a downstream upregulation of IFN-γ and IL-12, was also seen to be upregulated in samples taken from inflamed OcMMP eyes. This suggests a mediated-enhancement of cytotoxic activity of NK cells and $CD8^+$ cytotoxic T-lymphocytes, and inhibition of angiogenic activity, which may have otherwise been stimulated via other upregulated genes in the PDGF signaling pathway. SPP1 specifically, has also been shown to have prognostic value in mucosal neoplasia and fibrogenic macrophage subset induced inflammation [51,52].

Conjunctival inflammation was correlated with downregulation of RNF152, EEF2K, and TCF7L1. [42-442–44]RNF152 expression has been described to potentiate TLR and IL-1R- via MyD88 activation. TCF7L1 encodes a member of the T cell factor/lymphoid enhancer factor family of transcription factors, is antagonized by transforming growth factor beta (TGF-β), a key regulator of inflammatory and fibrotic responses. Upregulation of PSMC3, PANX1, NPC1 and OCLN negatively correlated with inflammation [35–39]. The expression of PANX1 in OcMMP eyes correlated with increased clinical inflammation score. PANX1 is associated with upregulation of the non-inflammatory apoptotic pathway yields in lower levels of visible conjunctival inflammation. OCLN, is an integral membrane protein necessary for cytokine-induced regulation of the tight junction paracellular permeability barrier and appears to inhibit regulation of epithelial inflammation and hyperplasia. Both these genes may be indicative of epithelia repair following inflammation and restoration of the conjunctival mucosal barrier. Furthermore, Insulin-like growth factor (IGF-1, known to be involved in epithelial cell migration) [53] was strongly downregulated in all OcMMP eyes versus controls and may underpin delayed healing of conjunctival ulcers seen in severe active OcMMP.

PSMC3 encodes a protein that processes ubiquitin-modified proteins intracellularly [35]. NPC1 upregulation is associated with glycolysis and lipogenesis, and prevents abnormal accumulation and intracellular storage or cholesterol and lipid [37]. Our data also showed upregulation of genes associated with lipid metabolism in OcMMP eyes. This included angiopoietin like 4 (ANGPTL4), a gene known to also encode for an apoptosis survival factor is upregulated in OcMMP eyes. This, along with an upregulation of LDL receptor related protein 1 (LRP1), a protein receptor associated with clearance of apoptotic cells, may suggest the presence of a biological response to counteract an increased apoptotic drive present on the ocular surface of inflamed OcMMP eyes. Collectively, these data indicate that analyses of pathways supporting conjunctival homeostasis in health and cicatricial conjunctival disease is complex.

Our data indicates that innate immune responses are key to the pathogenesis of human disease. Detailed analyses of the cytokine 'fingerprint' data show a reduction in genes associated with the adaptive immune response and an increase in innate markers regardless of inflammation, and break down of mucosal epithelial barrier function. Conversely, type 1 interferon genes are increased in samples from non-inflamed eyes. Our previous analyses of conjunctival cellular profiles [12,54,55] showed eyes with no visible inflammation and raised conjunctival neutrophils were more likely to progress, and have a greater degree of conjunctival shrinkage compared to those without raised neutrophils. Links between Type 1 interferon and neutrophils have been reported in conditions such as SLE and may be relevant here.

In summary, we have shown that Nanostring technology allows global gene expression data to be obtained from a simple conjunctival swab generating a transcriptome for OcMMP related to inflammation, extracellular matrix production, scarring sequelae, and epithelial barrier dysfunction. Gene associations with clinically scored patient symptomatology (OSDI®) and conjunctival inflammation (graded against a validated scoring system (CCAT©)) show a complex pattern incorporating fibrosis, immune responses, epithelial barrier integrity and molecular homeostasis. While these data are a based on a single sampling from patients and controls without confirmatory qPCR or protein analyses, the non-invasive sampling technique looks promising for use in future longitudinal disease-course studies and early-phase clinical trials of novel interventions. These studies will enable better understanding of the mechanism of conjunctival fibrosis in OcMMP, response to therapy, and provide new targets for anti-fibrotic agents, for which there is an unmet clinical need.

Financial support

This work was supported by Fight for Sight/National Eye Research Centre Small Grant Award Ref: 24NE182 and the UKRI Medical Research Council Experimental Medicine Award Ref MR/X019195/1.

Open access data resource

- https://www.rosalind.bio/
- Interpro: https://www.ebi.ac.uk/interpro/
- NCBI: https://pubchem.ncbi.nlm.nih.gov/docs/pathways
- MSigDB: https://www.gsea-msigdb.org/gsea/msigdb
- REACTOME: https://reactome.org/
- WikiPathways: https://www.wikipathways.org/search.html

Declaration of competing interest

None Declared.

Appendix A. Supplementary data

Supplementary data to this article can be found online at https://doi.org/10.1016/j.jtos.2023.09.005.

References

[1] Williams GP, Radford C, Nightingale P, et al. Evaluation of early and late presentation of patients with ocular mucous membrane pemphigoid to two major tertiary referral hospitals in the United Kingdom. Eye 2011;25(9):1207–18.
[2] Saw VPJ, Dart JKG, Rauz S, et al. Immunosuppressive therapy for ocular mucous membrane pemphigoid: strategies and outcomes. Ophthalmology 2008;115(2):253–61.
[3] Hübner F, Recke A, Zillikens D, et al. Prevalence and age distribution of pemphigus and pemphigoid diseases in Germany. J Invest Dermatol 2016;136(12):2495–8.
[4] Radford CF, Rauz S, Williams GP, et al. Incidence, presenting features, and diagnosis of cicatrising conjunctivitis in the United Kingdom. Eye 2012;26(9):1199–208.
[5] Cifuentes-González C, Amaris-Martínez S, Reyes-Guanes J, et al. Incidence, prevalence, and demographic characteristics of ocular cicatricial pemphigoid in Colombia: data from the National Health Registry 2009-2019. Int J Ophthalmol 2021;14(11):1765–70.
[6] Rauz S, Maddison PG, Dart JKG. Evaluation of mucous membrane pemphigoid with ocular involvement in young patients. Ophthalmology 2005;112(7):1268–74.
[7] Ong HS, Setterfield JF, Minassian DC, et al. Mucous membrane pemphigoid with ocular involvement: the clinical phenotype and its relationship to direct immunofluorescence findings. Ophthalmology 2018;125(4):496–504.
[8] Rashid H, Lamberts A, Borradori L, et al. European guidelines (S3) on diagnosis and management of mucous membrane pemphigoid, initiated by the European Academy of Dermatology and Venereology - Part I. J Eur Acad Dermatol Venereol 2021;35(9):1750–64.
[9] Schmidt E, Rashid H, Marzano AV, et al. European Guidelines (S3) on diagnosis and management of mucous membrane pemphigoid, initiated by the European Academy of Dermatology and Venereology - Part II. J Eur Acad Dermatol Venereol 2021;35(10):1926–48.
[10] Dart JK. The 2016 Bowman Lecture Conjunctival curses: scarring conjunctivitis 30 years on. Eye 2017;31(3):301–32.
[11] Ahadome SD, Mathew R, Reyes NJ, et al. Classical dendritic cells mediate fibrosis directly via the retinoic acid pathway in severe eye allergy. JCI Insight 2016;1(12).
[12] Williams GP, Nightingale P, Southworth S, et al. Conjunctival neutrophils predict progressive scarring in ocular mucous membrane PemphigoidImpression cytology for detecting biomarkers in OcMMP. Invest Ophthalmol Vis Sci 2016;57(13):5457–69.
[13] Saw VPJ, Dart RJC, Galatowicz G, et al. Tumor necrosis factor-α in ocular mucous membrane pemphigoid and its effect on conjunctival fibroblasts. Invest Ophthalmol Vis Sci 2009;50(11):5310–7.
[14] Saw VPJ, Offiah I, Dart RJ, et al. Conjunctival interleukin-13 expression in mucous membrane pemphigoid and functional effects of interleukin-13 on conjunctival fibroblasts in vitro. Am J Pathol 2009;175(6):2406–15.
[15] Ahadome SD, Abraham DJ, Rayapureddi S, et al. Aldehyde dehydrogenase inhibition blocks mucosal fibrosis in human and mouse ocular scarring. JCI Insight 2016;1(12).
[16] Saw VP, Schmidt E, Offiah I, et al. Profibrotic phenotype of conjunctival fibroblasts from mucous membrane pemphigoid. Am J Pathol 2011;178(1):187–97.
[17] Micera A, Stampachiacchiere B, Di Zazzo A, et al. NGF modulates trkANGFR/p75NTR in αSMA-expressing conjunctival fibroblasts from human ocular cicatricial pemphigoid (OCP). PLoS One 2015;10(11):e0142737.
[18] Ong HS, Minassian D, Rauz S, et al. Validation of a clinical assessment tool for cicatrising conjunctivitis. Ocul Surf 2020;18(1):121–9.
[19] Whitcher JP, Shiboski CH, Shiboski SC, et al. A simplified quantitative method for assessing keratoconjunctivitis sicca from the sjögren's syndrome international registry. Am J Ophthalmol 2010;149(3):405–15.
[20] Mitchell AL, Attwood TK, Babbitt PC, et al. InterPro in 2019: improving coverage, classification and access to protein sequence annotations. Nucleic Acids Res 2019;47(D1). D351-d60.
[21] Geer LY, Marchler-Bauer A, Geer RC, et al. The NCBI BioSystems database. Nucleic Acids Res 2010;38(Database issue):D492–6.
[22] Subramanian A, Tamayo P, Mootha VK, et al. Gene set enrichment analysis: a knowledge-based approach for interpreting genome-wide expression profiles. Proc Natl Acad Sci U S A 2005;102(43):15545–50.
[23] Liberzon A, Subramanian A, Pinchback R, et al. Molecular signatures database (MSigDB) 3.0. Bioinformatics 2011;27(12):1739–40.
[24] Fabregat A, Jupe S, Matthews L, et al. The reactome pathway knowledgebase. Nucleic Acids Res 2018;46(D1). D649-d55.
[25] Slenter DN, Kutmon M, Hanspers K, et al. WikiPathways: a multifaceted pathway database bridging metabolomics to other omics research. Nucleic Acids Res 2018;46(D1). D661-d7.
[26] de Paiva CS, Trujillo-Vargas CM, Schaefer L, et al. Differentially expressed gene pathways in the conjunctiva of sjögren syndrome keratoconjunctivitis sicca. Front Immunol 2021;12(2862).
[27] Afshari NA, Igo Jr RP, Morris NJ, et al. Genome-wide association study identifies three novel loci in Fuchs endothelial corneal dystrophy. Nat Commun 2017;8:14898.
[28] Karsenty G, Park RW. Regulation of type I collagen genes expression. Int Rev Immunol 1995;12(2–4):177–85.
[29] Kurioka A, Cosgrove C, Simoni Y, et al. CD161 defines a functionally distinct subset of pro-inflammatory natural killer cells. Front Immunol 2018;9:486.
[30] Kamperschroer C, Swain SL, Grussenmeyer T, Lefkovits I. SAP deficiency results in a striking alteration of the protein profile in activated CD4 T cells. J Proteome Res 2006;5(7):1785–91.
[31] Li P, Morris DL, Willcox BE, et al. Complex structure of the activating immunoreceptor NKG2D and its MHC class I–like ligand MICA. Nat Immunol 2001;2(5):443–51.
[32] Martini G, Cabrelle A, Calabrese F, et al. CXCR6-CXCL16 interaction in the pathogenesis of juvenile idiopathic arthritis. Clin Immunol 2008;129(2):268–76.
[33] Call ME, Pyrdol J, Wiedmann M, Wucherpfennig KW. The organizing principle in the formation of the T cell receptor-CD3 complex. Cell 2002;111(7):967–79.
[34] Lignitto L, Carlucci A, Sepe M, et al. Control of PKA stability and signalling by the RING ligase praja2. Nat Cell Biol 2011;13(4):412–22.
[35] Kröll-Hermi A, Ebstein F, Stoetzel C, et al. Proteasome subunit PSMC3 variants cause neurosensory syndrome combining deafness and cataract due to proteotoxic stress. EMBO Mol Med 2020;12(7):e11861.
[36] Bruzzone R, Hormuzdi SG, Barbe MT, et al. Pannexins, a family of gap junction proteins expressed in brain. Proc Natl Acad Sci U S A 2003;100(23):13644–9.
[37] Kwon HJ, Abi-Mosleh L, Wang ML, et al. Structure of N-terminal domain of NPC1 reveals distinct subdomains for binding and transfer of cholesterol. Cell 2009;137(7):1213–24.
[38] Elias BC, Suzuki T, Seth A, et al. Phosphorylation of Tyr-398 and Tyr-402 in occludin prevents its interaction with ZO-1 and destabilizes its assembly at the tight junctions. J Biol Chem 2009;284(3):1559–69.
[39] Romero V, Azocar J, Zúñiga J, et al. Interaction of NK inhibitory receptor genes with HLA-C and MHC class II alleles in Hepatitis C virus infection outcome. Mol Immunol 2008;45(9):2429–36.
[40] Zhang S, Wu W, Wu Y, et al. RNF152, a novel lysosome localized E3 ligase with pro-apoptotic activities. Protein Cell 2010;1(7):656–63.
[41] Browne GJ, Proud CG. A novel mTOR-regulated phosphorylation site in elongation factor 2 kinase modulates the activity of the kinase and its binding to calmodulin. Mol Cell Biol 2004;24(7):2986–97.
[42] Kim TW, Kim HJ, Lee C, et al. Identification of replicative senescence-associated genes in human umbilical vein endothelial cells by an annealing control primer system. Exp Gerontol 2008;43(4):286–95.
[43] Yu Z, Joy S, Mi T, et al. New, potent, small molecule agonists of tyrosine kinase receptors attenuate dry eye disease. Front Med 2022;9:937142.
[44] Alam J, de Paiva CS, Pflugfelder SC. Desiccation induced conjunctival monocyte recruitment and activation - implications for keratoconjunctivitis. Front Immunol 2021;12:701415.
[45] Kessal K, Daull P, Cimbolini N, et al. Comparison of two experimental mouse dry eye models through inflammatory gene set enrichment analysis based on a multiplexed transcriptomic approach. Int J Mol Sci 2021;22(19).
[46] Liang H, Kessal K, Rabut G, et al. Correlation of clinical symptoms and signs with conjunctival gene expression in primary Sjögren syndrome dry eye patients. Ocul Surf 2019;17(3):516–25.
[47] Dutt JE, Ledoux D, Baer H, Foster CS. Collagen abnormalities in conjunctiva of patients with cicatricial pemphigoid. Cornea 1996;15(6):606–11.
[48] Razzaque MS, Foster CS, Ahmed AR. Role of collagen binding heat shock protein 47 and transforming growth factor-β1 in conjunctival scarring in ocular cicatricial pemphigoid. Invest Ophthalmol Vis Sci 2003;44:1616–21.
[49] Bernauer W, Wright P, Dart JKG, et al. The conjunctiva in acute and chronic mucous membrane pemphigoid. Ophthalmology 1993;100:339–46.
[50] Elder MJ, Dart JKG, Lightman S. Conjunctival fibrosis in ocular cicatricial pemphigoid - the role of cytokines. Br J Ophthalmol 1997;65:165–76.
[51] Li X, Zhang Q, Chen G, Luo D. Multi-Omics analysis showed the clinical value of gene signatures of C1QC(+) and SPP1(+) TAMs in cervical cancer. Front Immunol 2021;12:694801.
[52] Fabre T, Barron AMS, Christensen SM, et al. Identification of a broadly fibrogenic macrophage subset induced by type 3 inflammation. Sci Immunol 2023;8(82):eadd8945.
[53] Yamada N, Matsuda R, Morishige N, et al. Open clinical study of eye-drops containing tetrapeptides derived from substance P and insulin-like growth factor-1 for treatment of persistent corneal epithelial defects associated with neurotrophic keratopathy. Br J Ophthalmol 2008;92(7):896–900.
[54] Williams GP, Denniston AK, Oswal KS, et al. The dominant human conjunctival epithelial CD8αβ+ T cell population is maintained with age but the number of CD4 + T cells increases. Age 2012;34(6):1517–28.
[55] Wlliams GP, Tomlins PJ, Denniston AK, et al. Elevation of conjunctival epithelial CD45INTCD11b+CD16+CD14- neutrophils in ocular stevens-johnson syndrome and toxic epidermal necrolysis. Invest Ophthalmol Vis Sci 2013. https://doi.org/10.1167/iovs.13-11859.